文章编号:0253-2778(2019)12-1010-08

Chemically responsive charge transfer plasmon for glucose detection

HUANG Shan[1], ZHU Yujun[2]

(1. *Department of Chemistry, University of Science and Technology of China, Hefei* 230026, *China*;
2. *Department of Chemical and Chemical Engineering, Hefei Normal University, Hefei* 230601, *China*)

Abstract: Au-Ag bimetallic plasmonic nanostructures were successfully prepared by introducing silver into the nano gap of the gold nanoparticles(AuNPs) dimer based on the silver ion soldering method and the seed-mediated growth method. Due to the etching effect of H_2O_2 on the silver conductive junction which was formed by enzymatic oxidation of glucose, the charge transfer plasmon (CTP) would have a good response to glucose. Based on this, it could be applied to the detection of glucose. The relationship between glucose concentration and the intensity, wavelength of CTP peak, and surface enhanced Raman spectroscopy (SERS) intensity, as well as the selectivity of the sensor were investigated. The experimental results show that the method has high sensitivity and good selectivity towards glucose. Two linear relationships were identified between the CTP peak intensity change value and the glucose concentration in the range of 0.5～4 μmol/L and 4～10 μmol/L, respectively, with a limit of detection (3σ rule) reaching 0.2 μmol/L. The naked-eye detection of glucose can reach the micromolar level. The SERS also exhibited a linear response toward glucose, within the concentration range of 1～10 μmol/L.

Key words: plasmonic nanostructure; charge transfer plasmon; optical sensing; glucose

CLC number: O65 **Document code**: A doi:10.3969/j.issn.0253-2778.2019.12.008

Citation: HUANG Shan, ZHU Yujun. Chemically responsive charge transfer plasmon for glucose detection[J]. Journal of University of Science and Technology of China, 2019,49(12):1010-1017.
黄珊,朱玉俊. 用于葡萄糖检测的化学响应电荷转移等离激元[J]. 中国科学技术大学学报,2019,49(12):1010-1017.

用于葡萄糖检测的化学响应电荷转移等离激元

黄 珊[1], 朱玉俊[2]

(1. 中国科学技术大学化学系, 安徽合肥 230026;
2. 合肥师范学院化学与化学工程学院, 安徽合肥 230601)

摘要: 基于银离子焊接法和种子生长法,在金纳米二聚体的粒间间隙处引入银,成功制备了金-银双金属等离激元纳米结构. 由于葡萄糖的酶促触发氧化反应产生的 H_2O_2 对银导电结点的蚀刻作用,该结构的电荷转移等离激元(CTP)对葡萄糖有很好的响应,基于此,可将其应用于葡萄糖的检测. 主要研究了葡萄糖浓度与CTP峰强度、波长和表面增强拉曼光谱(SERS)强度之间的关系,以及传感器的选择性. 实验结果表明,该方

Received: 2019-04-29; **Revised**: 2019-05-31
Foundation item: Supported by National Natural Science Foundation of China (21521001).
Biography: HUANG Shan, female, born in 1994, master. Research field: nanoanalytical chemistry. E-mail: hs12@mail.ustc.edu.cn
Corresponding author: ZHU Yujun, PhD. E-mail: zyj8119@sina.com

法灵敏度高、选择性好；葡萄糖浓度分别在 0.5～4 mol/L 和 4～10 μmol/L 两个浓度范围内与 CTP 强度变化值存在线性关系，检测限(3σ 法)为 0.2 μmol/L；并且，肉眼检测葡萄糖可以达到微摩尔水平；SERS 信号变化值与葡萄糖浓度在 1～10 μmol/L 范围内也存在很好的线性关系.

关键词：等离激元纳米结构；电荷转移等离激元；光学传感；葡萄糖

0 Introduction

Diabetes mellitus (DM) is a chronic metabolic disorders that poses a serious threat to human health[1-2]. According to the World Health Organization, 451 million people worldwide had diabetes in 2017, and these numbers are expected to increase to 693 million by 2045[3]. It is known that elevated glucose level in blood is a reliable indicator for diabetes. Therefore, it is necessary to explore a simple, effective and sensitive measurement method to detect glucose concentration[4-6].

In recent years, a variety of nanomaterials have been developed for use in the detection of glucose, for example, Fe_3O_4 magnetic nanoparticles[7], nitrogen-doped graphene quantum dots[8] and CuS nanoparticles[9]. In addition, gold and silver nanoparticles have also been widely used in optical sensing to detect glucose[10-12]. There are several general strategies for glucose sensing: local surface plasmon resonance (LSPR) peak drifts or extinction spectral intensity variation[13], surface enhanced Raman spectroscopy (SERS)[14], and fluorometric methods[15], wherein the measurement based on the former two has the advantages of simple operation and high sensitivity, and which are rarely combined in the current research.

In this work, a dual-mode sensors based on colorimetric and SERS methods are designed for H_2O_2-mediated glucose detection. Au dimer@Ag bimetallic plasmonic nanostructure was successfully constructed and a conductive junction was formed by silver deposition, resulting in a CTP resonance mode, which is responsive to the etching of Ag by H_2O_2 produced by catalytic oxidation of glucose.

1 Experimental

1.1 Materials and instruments

Chloroauric acid tetrahydrate ($HAuCl_4 \cdot 4H_2O$) and hydrogen peroxide were obtained from Sinopharm Chemical Reagent Co., Ltd. (Shanghai, China). Fish sperm DNA (FSDNA) and sodium citrate tribasic dihydrate were bought from Sigma. $AgNO_3$ was obtained from Bio Basic Inc. (BBI, Canada); bis (p-sulfonatophenyl) phenylphosphine dihydrate dipotassium salt (BSPP) was a product of Strem Chemical (Newburyport, MA, USA). Glucose oxidase (GOx, 50 kU) was obtained from Sangon Bioengineering Technology and Services Co., Ltd (Shanghai, China). Glucose was purchased from Sinopharm Chemical Reagent Co., Ltd. α-Lactose, D-fructose, maltose, sucrose were ordered by Shanghai Shenggong Bioengineering Technology Service Co., Ltd. 4-nitrophenol (4-NTP) was purchased from J&K Chemicals (Beijing, China). All the reagents were used as received without further purification.

The following instruments were used in our experiments: U-2910 Hitachi UV-Vis spectrophotometer (Hitachi, Japan), 7700 Transmission Electron Microscope (Hitachi, Japan), Portable Raman spectrometer (US Ocean Optical Raman system, Maya 2000 CCD detector, with incident laser wavelength set at 671 nm).

1.2 Preparation of gold nanoparticles, AuNP dimers and Au dimer@Ag

AuNPs (gold nanoparticles) with different diameters were synthesized by seed-growth method as reported before[16]. The resulting citrate-terminated nanoparticles were interacted with BSPP at room temperature to complete a ligand exchange. The BSPP-covered AuNPs were

collected by centrifugation and redispersed in deionized H_2O.

The BSPP-modified AuNPs was added to 0.5 ×TBE (pH 8.0; 44.5 mmol/L Tris, 1 mmol/L EDTA, 44.5mmol/L boric acid) buffer at room temperature, then $AgNO_3$ and 0.5 μg/μL FSDNA were added. The resulting discrete AuNP clusters were then separated by agarose gel electrophoresis to obtain a dimeric assembly product[17].

The deposition of Ag on the AuNP dimers was carried out by a seed-mediated growth method just reported by our group[18]. 20 μL of 38.8 mmol/L sodium citrate and different volumes of 1 mmol/L $AgNO_3$ were added to 1mL of boiling water containing 0.1nmol/L AuNPs dimers. The solution was kept boiling for 20 min in an oil bath at 125℃ to obtain Au dimer @ Ag products. According to the reported work by our group[17-18], we used Au dimer@Ag based on 25 nm and 32nm for colorimetic assay and SERS assay, respectively.

1.3 H_2O_2 etching of Au dimer@Ag

Different concentrations of H_2O_2 were added to an aqueous solution of Au dimer @ Ag (0.06 nmol/L) and incubated at 37℃ for 2.5h to complete the etching reaction.

1.4 UV-Vis, naked-eye and SERS detection of glucose

UV-Vis detection of glucose was performed in the following steps: ①different concentrations of glucose (from 0 to 25 μmol/L) were respectively incubated with glucose oxidase (GOx, 500 μg/mL) at 37℃ for 30 min; ② after incubation, prepared Au dimer @ Ag (0.06 nmol/L) were introduced into the solution and the final volume was 200 μL. The extinction spectra after 2.5 h was measured. Herein, we used AuNPs with particle size of 25 nm to prepare Au dimer@Ag structure.

For the naked-eye detection of glucose, the final concentration of Au dimer @ Ag was 0.1 nmol/L. At this concentration, the color of the solution after the reaction was more pronounced. And the glucose concentration varied between 0～30 μmol/L.

For the SERS detection of glucose, we used AuNPs with a particle size of 32nm to prepare dimers, and the final concentration of Au dimer@Ag used was 0.1 nmol/L. After mixing 1×10^{-2} mol/L 4-NTP and 10 mmol/L TCEP in equal volume, the solution was quickly added to the reaction solution and incubated for 30 min, and the final concentration of 4-NTP was 1×10^{-4} mol/L, followed by the SERS detection. Laser wavelength was set at 671 nm.

2 Results

2.1 Characterization of Au dimer@Ag

Fig.1(a) and (b) are TEM images of AuNP dimers and Au dimer @ Ag, respectively. Compared with AuNPs dimers, the gaps between two AuNPs in the Au dimer @ Ag disappeared because they are filled with Ag (Fig.1(b)). The TEM image also demonstrated the monodispersibility of Au dimer @ Ag. As illustrated in Fig.1(c), AuNP dimers showed two LSPR peaks at ～ 520nm and ～ 650nm, corresponding to the transverse and longitudinal resonance modes, respectively. After deposition of Ag, the transverse LSPR peak slightly blue shifted compared to Au NPs dimers, meanwhile the longitudinal LSPR redshifted. These could be attributed to the CTP mode enabled by bridging the conductive junction (CJ) of the two AuNPs[19-20]. Moreover, the extinction spectra of Au dimer@Ag overlap perfectly after 14 days of storage (Fig.1(d)), which indicates that they have outstanding stability due to the protective effect of citrate used during the Ag deposition process.

2.2 Etching of Au dimer@Ag by H_2O_2

It can be seen fromFig.2(a),(b) that after the adding excess H_2O_2, the CJ width in the Au dimer @Ag structure was significantly reduced, which was due to the oxidative etching of Ag. And Fig.2(c) showed the extinction spectrum of Au dimer@Ag under different concentrations of H_2O_2. With the increasing concentration of H_2O_2, the CTP

peak at ～700 nm of Au dimer@Ag gradually redshifted and the intensity gradually decreased. When the concentration of H_2O_2 was increased to 8μmol/L, another peak emerged at ～630 nm. The electron conduction efficiency was lowered due to the narrowing of the silver CJ width, there was an opposite local net charge on the surface where the two AuNPs are close to each other. Therefore, the capacitive coupling resonance mode became pronounced which resulted in the new peak[21-22].

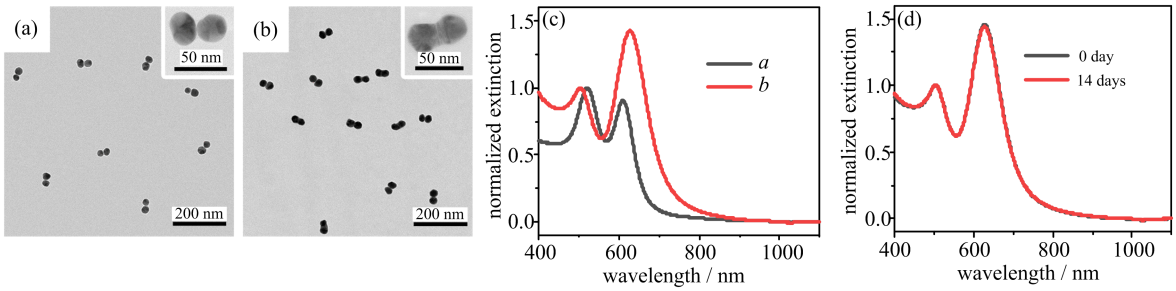

(a) TEM images of the AuNPs dimer before Ag depositions; (b) TEM images of the AuNPs dimer after Ag depositions; insets are high-magnification TEM images; (c) Extinction spectra of (a-b); (d) Extinction spectra of Au dimer@Ag at different storage time.

Fig. 1　Characterization of Au dimer@Ag

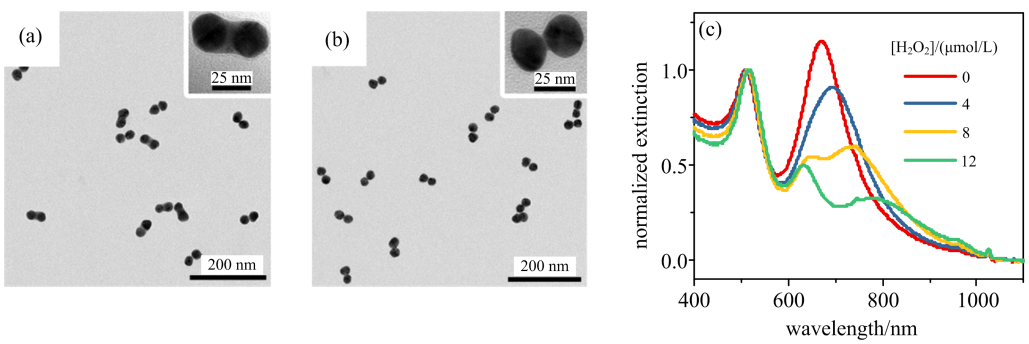

(a) TEM images of the Au dimer@Ag before etching by 40 μmol/L H_2O_2; (b) TEM images of the Au dimer@Ag after etching by 40 μmol/L H_2O_2; insets are high-magnification TEM images; (c) Extinction spectra of Au dimer@Ag treated with different concentrations of H_2O_2 from 0 ～ 12 μmol/L.

Fig. 2　TEM images and extinction spectra of Au dimer@Ag etched by H_2O_2

2.3　UV-Vis detection of glucose

In the presence of glucose oxidase, glucose can be reduced, which produces H_2O_2. And the entire reaction process can be described by Equations (1) and (2)[23]:

$$O_2 + \text{glucose} \xrightarrow{\text{GOx}} H_2O_2 + \text{gluconic acid} \quad (1)$$

$$2Ag + H_2O_2 \rightarrow 2Ag^+ + 2OH^- \quad (2)$$

Here, the Au dimer@Ag samples were reacted with different concentrations (0.5～25 μmol/L) of glucose with glucose oxidase, and the extinction spectrum of the sample solution was measured after the reaction to obtain Fig. 3(a). As a result, the CTP peaks of the Au dimer@Ag gradually redshifted as the glucose concentration increased, while the intensity of the peaks decreased. Fig. 3 (b) showed that the change of CTP peak intensity increased with the increasing glucose concentration. The change in peak intensity reached plateau after the glucose concentration was increasedto 15μmol/L, which was mainly caused by the depletion of Ag CJ.

Moreover, we can get two standard curves from the above figure. The linear regression equation in the glucose concentration range of 0.5～4 μmol/L was $(A_0 - A_t) = -0.176\,2 + 0.130\,53\,c/(\mu\text{mol/L})$ ($R^2 = 0.995$), and the linear regression equation in the glucose concentration range of 4～10 μmol/L was $(A_0 - A_t) = 0.197\,75 + 0.077\,12\,c/(\mu\text{mol/L})$ ($R^2 = 0.991$). The slopes of the two standard curves were different, which is due to the complication of capacitive coupling resonance mode to the plasmonic peak. As shown

in Fig. 2(c), when the glucose concentration was less than 4μmol/L, only the CTP mode existed because the Ag CJ was sufficiently wide. However when the concentration of glucose was further increased, besides the CTP mode, the capacitive coupling resonance mode at around 650nm was observed, so the slope of the latter working curve would decrease.

To verify that the effect of glucose on the extinction spectrum of Au dimer@Ag was due to the formation of H_2O_2 in the presence of glucose oxidase, the Au dimer@Ag samples after reacting with different concentrations of glucose were characterized by TEM.

As shown in Fig. 4, as the glucose concentration increased, the CJ widths of Au dimer@Ag were 19 nm ±0.7 nm, 14.5 nm±0.2 nm and 11.9 nm±0.1 nm with 0, 10 μmol/L, and 30 μmol/L glucose, respectively. The CJ width was reduced because the deposited silver was gradually etched.

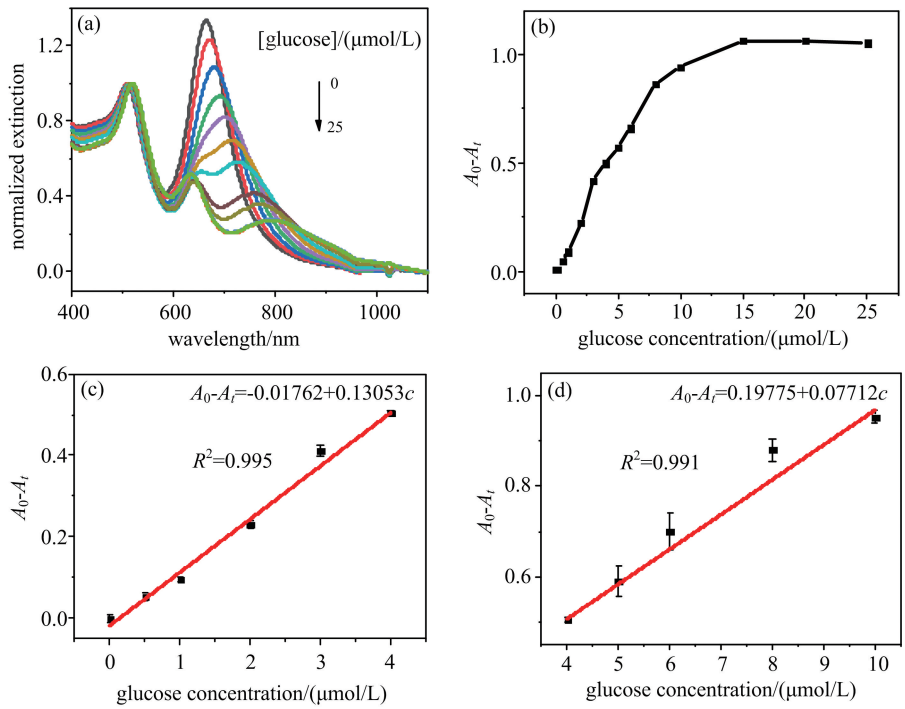

(a) Extinction spectra of Au dimer@Ag samples treated with different concentrations of glucose from 0 to 25 μmol/L; (b) absorption value change of Au dimer@Ag in the presence of 0, 0.5, 1, 2, 3, 4, 5, 6, 8, 10, 15, 20 and 25 μmol/L glucose; two linear calibration graphs by plotting the absorbance change value vs glucose concentration within (c) 0.0～4.0μmol/L and (d) 4.0～10μmol/L

Fig. 3 Quantitative assays of Au dimer@Ag by UV-Vis detection

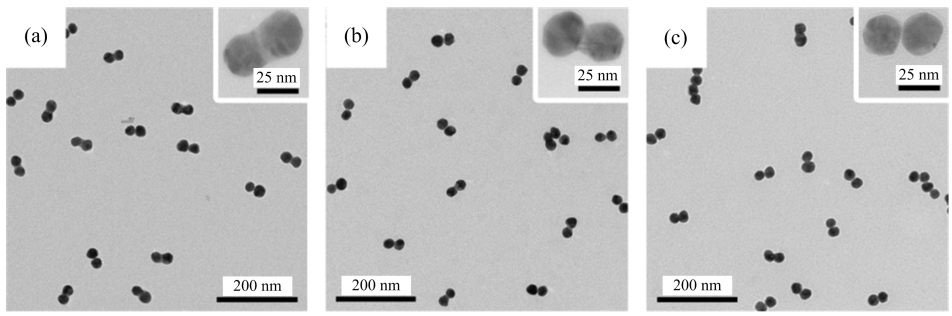

Insets are the high-magnification TEM images. Concentrations of glucose in (a-c) were 0, 10 and 30 μmol/L, respectively

Fig. 4 TEM images of the Au dimer@Ag treated with different concentrations of glucose

2.4 Naked-eye detection of glucose

Due to the wide range of wavelength changes caused by etching, the naked-eye detection of glucose could be achieved by vivid color changes. As shown in Fig. 5, the glucose concentration was varied between 0 and 30 μmol/L, and the color of

the solution changed from green to brown and then to red after the reaction, which was easily distinguished with the naked-eye. It can be seen that when the glucose concentration was as low as 10 μmol/L, there was already a very significant color change.

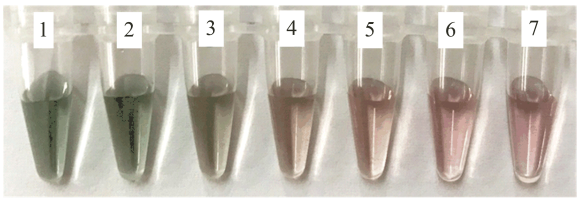

Fig. 5　Photograph of Au dimer@Ag solution treated with 0, 5, 10, 15, 20, 25 and 30 μmol/L glucose, corresponding to 1～7 respectively

2.5　SERS detection of glucose

Fig. 6(a) showed the Raman spectra of Au dimer @ Ag after reacting with different concentrations of glucose. The SERS intensity increased with increasing glucose concentration. The gap between the AuNPs formed a SERS hot spot, as the glucose concentration increased, the silver was etched, and the hot spot was gradually exposed, so there would be more signal molecules (4-NTP) combined with the hot spot, which was consistent with the increasing SERS intensity[24]. Fig. 6(b) showed the relationship between the characteristic peak intensity change of 4-NTP at 1 330 cm^{-1} and the glucose concentration. When the concentration was less than 15μmol/L, the SERS signal changes linearly with the glucose concentration. When the glucose concentration was further increased, since the silver was almost completely etched, the SERS intensity would not change any more. And the linear regression equation in the glucose concentration range of 1～10 μmol/L was $\Delta I = 556.77\ c/(\mu mol/L)$ ($R^2 = 0.998$), which showed a good linear relationship. The LOD was 1.16 μmol/L (3σ rule). As shown in Tab. 1, compared with other methods, the proposed optical sensor based on colormetry and SERS method herein exhibits a lower LOD, indicating a great potential for practical applications.

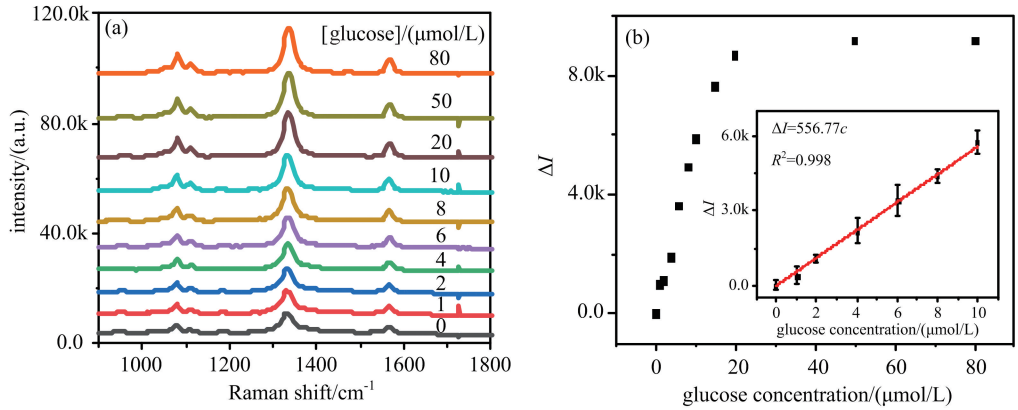

(a) Raman spectra of Au dimer@Ag samples treated with different concentrations of glucose from 0～80μmol/L; (b) SERS intensity change of 4-NTP at 1330cm^{-1} in the presence of 0, 1, 2, 4, 6, 8, 10, 20, 50 and 80 μmol/L. Inset: plot of linear region from 1～10 μmol/L

Fig. 6　Quantitative assays of Au dimer@Ag by SERS detection

Tab. 1　Comparisons with other methods for determination of glucose

Nanomaterials	Method	Linear range/(μmol/L)	LOD/(μmol/L)	Referance
Au@Ag core-shell NPs	Colorimetry	0.5～400	0.24	[25]
BCQDs	Fluorometry	8～80	8.0	[26]
$MnCo_2O_4$ NFs	Electrochemistry	0.05～800	10	[27]
Ag@AuNPs/GO	SERS	2000～6000	330	[28]
Au dimer@Ag	Colorimetry	0.5～4, 4～10	0.2	This work
	SERS	1～10	1.16	

[Note] BCQDs: B-doped carbon quantum dots; NFs: nanofibers, GO: graphene oxide.

2.6 The study of sensor selectivity

To verify the specificity of Au dimer@Ag for glucose response, 20 μmol/L glucose was selected for comparative studies with different monosaccharides and polysaccharides (α-lactose, D-fructose, sucrose and maltose). Each saccharide concentration was 10 times of the glucose concentration. As shown in Fig. 7, the designed sensor had a very good selectivity for glucose detection and almost no response to other sugars, thereby demonstrating its high selectivity and specificity for glucose response.

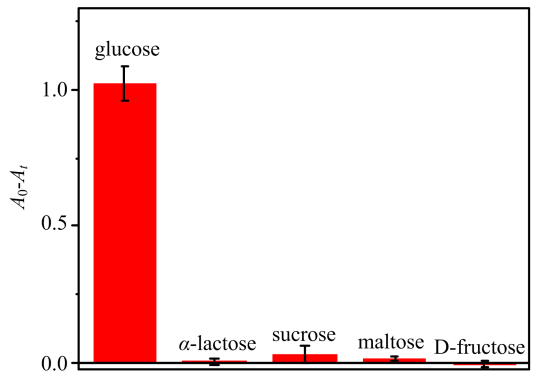

Fig. 7 Sensor selectivity test of Au dimer@Ag in the presence of 20 μmol/L glucose and other carbohydrates at a concentration of 200 μmol/L

3 Conclusion

In summary, we developed a dual-mode glucose detection strategy for colorimetric method and SERS by using Au dimer@Ag bimetallic plasmonic nanostructures as substrates. In this assay, glucose oxidase first catalyzed the oxidation of the glucose substrate to produce H_2O_2, which would further etch the silver deposited in the nano gap of the AuNP dimers. As a result, the CTP peak of the Au dimer@Ag decreased along with the color of the solution changed from green to brown and finally to red. Meanwhile, SERS signal also increased due to the exposed SERS hotspot after etching. Because of its excellent stability and low detection limit, Au dimer@Ag could be applied for glucose detection in various scenarios to different requirements in the future. Furthermore, the design strategies could also be applied to other nanostructures with different substrate and depositing metals.

References

[1] THORENS B. GLUT2, glucose sensing and glucose homeostasis[J]. Diabetologia, 2015, 58(2): 221-232.

[2] PANG Y J, HUANG Z L, YANG Y F, et al. Colorimetric detection of glucose based on ficin with peroxidase-like activity [J]. Spectrochim Acta A, 2018, 189: 510-515.

[3] CHO N H, SHAW J E, KARURANGA S, et al. IDF Diabetes Atlas: Global estimates of diabetes prevalence for 2017 and projections for 2045[J]. Diabetes Res Clin Pr, 2018,138: 271-281.

[4] DARABDHARA G, SHARMA B, DAS M R, et al. Cu-Ag bimetallic nanoparticles on reduced graphene oxide nanosheets as peroxidase mimic for glucose and ascorbic acid detection[J]. Sensor Actuat B-Chem, 2017, 238: 842-851.

[5] JIN L H, MENG Z, ZHANG Y Q, et al. Ultrasmall Pt nanoclusters as robust peroxidase mimics for colorimetric detection of glucose in human serum[J]. Acs Appl Mater Inter, 2017, 9(11): 10027-10033.

[6] CAMLI B, KUSAKCI E, LAFCI B, et al. Cost-effective microstrip antenna driven ring resonator microwave biosensor for biospecific detection of glucose[J]. IEEE J Sel Top Quant, 2017, 23(2): 404-409.

[7] WEI H, WANG E. Fe_3O_4 magnetic nanoparticles as peroxidase mimetics and their applications in H_2O_2 and glucose detection[J]. Anal Chem, 2008, 80(6): 2250-2254.

[8] HE Y, WANG X, SUN J, et al. Fluorescent blood glucose monitor by hemin-functionalized graphene quantum dots based sensing system[J]. Anal Chim Acta, 2014, 810(810C): 71-78.

[9] KARIKALAN N, KARTHIK R, CHEN S M, et al. Sonochemical synthesis of sulfur doped reduced graphene oxide supported CuS nanoparticles for the non-enzymatic glucose sensor applications [J]. Sci Rep, 2017, 7(1): 2494.

[10] TABRIZI M A, VARKANI J N. Green synthesis of reduced graphene oxide decorated with gold nanoparticles and its glucose sensing application[J]. Sensor Actuat B-Chem, 2014, 202(4): 475-482.

[11] FENG C, XU G, LIU H, et al. Glucose biosensors based on Ag nanoparticles modified TiO_2 nanotube arrays [J]. J Solid State Electr, 2014, 18(1): 163-171.

[12] HUANG P H, HONG C P, ZHU J F, et al. Ag@Au

nanoprism-metal organic framework-based paper for extending the glucose sensing range in human serum and urine[J]. Dalton T, 2017, 46(21): 6985-6993.

[13] LIN Y, ZHAO M, GUO Y, et al. Multicolor colormetric biosensor for the determination of glucose based on the etching of gold nanorods[J]. Sci Rep, 2016, 6: 37879.

[14] SUN D, QI G, XU S, et al. Construction of highly sensitive surface-enhanced Raman scattering (SERS) nanosensor aimed for the testing of glucose in urine [J]. Rsc Adv, 2016, 6(59): 53800-53803.

[15] MA J L, YIN B C, WU X, et al. Simple and cost-effective glucose detection based on carbon nanodots supported on silver nanoparticles[J]. Anal Chem, 2017, 89(2): 1323-1328.

[16] BASTUS N G, COMERNGE J, PUNTES V. Kinetically controlled seeded growth synthesis of citrate-stabilized gold nanoparticles of up to 200 nm: size focusing versus Ostwald ripening[J]. Langmuir, 2011, 27(17): 11098-11105.

[17] LIU M, FANG L, LI Y, et al. "Flash" preparation of strongly coupled metal nanoparticle clusters with sub-nm gaps by Ag^{+} soldering: toward effective plasmonic tuning of solution-assembled nanomaterials[J]. Chem Sci, 2016, 7(8): 5435-5440.

[18] WANG Y, FANG L, GONG M, et al. Chemically modified nanofoci unifying plasmonics and catalysis [J]. Chem Sci, 2019,10:5929-5934.

[19] HALAS N J, LAI S, CHANG W S, et al. Plasmons in strongly coupled metallic nanostructures[J]. Chem Rev, 2011, 111(6): 3913-3961.

[20] BORISSOV A. The quantum regime in tunneling plasmonics[J]. Nature, 2012, 491(7425): 574-577.

[21] ROMERO I, AIZPURUA J, BRYANT G W, et al. Plasmons in nearly touching metallic nanoparticles: singular response in the limit of touching dimers[J]. Opt Express, 2006, 14(21): 9988-9999.

[22] ATAY T, SONG J H, NURMIKKO A V. Strongly interacting plasmon nanoparticle pairs: from dipole-dipole interaction to conductively coupled regime[J]. Nano Lett, 2004, 4(9): 1627-1631.

[23] HE H, XU X, WU H, et al. In Situ Nanoplasmonic probing of enzymatic Activity of monolayer-confined glucose oxidase on colloidal nanoparticles[J]. Anal Chem, 2013, 85(9): 4546-4553.

[24] ALEXANDER K D, HAMPTON M J, ZHANG S, et al. A high-throughput method for controlled hot-spot fabrication in SERS-active gold nanoparticle dimer arrays[J]. J Raman Spectrosc, 2009, 40(12): 2171-2175.

[25] ZHANG X, MIN W, LV B, et al. Sensitive colorimetric detection of glucose and cholesterol by using Au@Ag core-shell nanoparticles[J]. Rsc Adv, 2016, 6(41): 35001-35007.

[26] SHAN X, CHAI L, MA J, et al. B-doped carbon quantum dots as a sensitive fluorescence probe for hydrogen peroxide and glucose detection[J] Analyst, 2014, 139(10): 2322-2325.

[27] ZHANG Y, LUO L, ZHANG Z, et al. Synthesis of MnCo2O4 nanofibers by electrospinning and calcination: application for a highly sensitive non-enzymatic glucose sensor[J]. J Mater Chem B, 2014, 2: 529-535.

[28] GUPTA V K, ATAR N, YOLA M L, et al. A novel glucose biosensor platform based on Ag @ AuNPs modified graphene oxide nanocomposite and SERS application[J]. J Colloid and Interface Sci, 2013, 406: 231-237.